AIP | Applied Physics Letters

Collision and dynamic frictional properties of boron nitride nanotubes

Xiaoming Chen, Meng Zheng, Cheol Park, and Changhong Ke

Citation: Appl. Phys. Lett. **102**, 121912 (2013); doi: 10.1063/1.4799489
View online: http://dx.doi.org/10.1063/1.4799489
View Table of Contents: http://apl.aip.org/resource/1/APPLAB/v102/i12
Published by the American Institute of Physics.

Collision and dynamic frictional properties of boron nitride nanotubes

Xiaoming Chen,[1,a)] Meng Zheng,[1,a)] Cheol Park,[2,3] and Changhong Ke[1,b)]
[1]*Department of Mechanical Engineering, State University of New York at Binghamton, Binghamton, New York 13902, USA*
[2]*National Institute of Aerospace, Hampton, Virginia 23666, USA*
[3]*Department of Mechanical and Aerospace Engineering, University of Virginia, Charlottesville, Virginia 22904, USA*

(Received 26 February 2013; accepted 20 March 2013; published online 29 March 2013)

Collision and dynamic frictional properties of boron nitride nanotubes (BNNTs) are of importance to their structural applications related to impact protection. In this paper, we present an experimental study of the lateral collision between moving atomic force microscopy probe tips and individual standstill BNNTs. Our results reveal that increasing the impact velocity results in a more prominent increase of the collision force at low velocity levels. This observation is ascribed to the opposite influences of the impact velocity on the dynamic frictional force and the contact angle on the tip-tube collision contact. © *2013 American Institute of Physics*. [http://dx.doi.org/10.1063/1.4799489]

Boron nitride nanotubes (BNNTs) are a highly crystalline, one-dimensional tubular nanostructure composed of partially ionic and hexagonal B-N bonding networks.[1,2] BNNTs are light-weight and possess high Young's modulus (~1 TPa) and strength (~30 GPa)[3–5] that are comparable to their pure carbon counterparts, carbon nanotubes (CNTs). Owning to their extraordinary chemical and thermal stabilities,[6,7] electrically insulating properties,[1,8] and excellent neutron absorbing capacity, BNNTs have become promising protective materials for a number of applications, ranging from encapsulating nanomaterials and devices[9] to building blocks for personal/vehicle armors and space shuttle shields. A full understanding of the mechanical properties of BNNTs under both static and dynamic loading conditions is essential to realizing their protection applications. Several recent studies have shed light on the mechanical properties of BNNTs in both longitudinal and lateral directions under quasi-static loading conditions.[3,4,10–12] However, their response to dynamic impact loads remains largely unexplored.

When a moving particle collides laterally with a nanotube, the resulting collision interaction is composed of the normal compression of the tube and the particle as well as their tangent frictional interactions. The collision can cause substantial traverse deformation in the nanotube, which may reach the plastic deformation regime[10] or, in a worse scenario, result in tube fracture.[13] Because the nanotube has a smooth surface with an angstrom level flatness, sliding of the particle on the nanotube surface may occur and thus reduce the impacting energy adsorbed by the nanotube. The collision interaction between the particle and the nanotube is expected to be affected by factors including the mass and velocity of the particle, the deformability of the particle and the nanotube, the frictional force on the particle-tube contact, and so on. In this paper, we present an experimental study on the collision of moving atomic force microscopy (AFM) probes that possess nearly semi-spherical tips with individual BNNTs that stand still on flat substrates, which is illustrated in Figure 1(a). The AFM tip is applied with a normal compressive load, P, against the substrate, and slides on the substrate at a constant velocity, V, until it impacts the nanotube. Our study focuses on quantifying the lateral collision force to the nanotube and the dynamic frictional force between the nanotube and the AFM tip as well as their respective dependences on the impact velocity.

Figure 1(b) shows the schematic illustration of our experimental scheme of measuring the lateral collision between an AFM probe tip and a BNNT. The motion of the AFM probe is controlled such that it collides laterally onto the BNNT with the tip moving in a direction perpendicular to the tube axis. A laser reflection scheme is employed to measure the normal and torsional deflections of the AFM cantilever. These deflection measurements are used to plot the nanotube topography profile and to calculate the lateral force applied to the AFM tip, respectively. When the AFM tip only slides on the substrate surface, the torsional deflection of the AFM cantilever results from the frictional force between the AFM tip and the substrate. After the AFM tip collides onto the nanotube surface, the resulting lateral collision force increases the torsional deflection of the AFM cantilever. When the AFM tip slides right on top of the nanotube, the torsional deflection of the AFM cantilever is caused purely by the frictional force on the tip-tube contact.

The employed BNNTs in this study were synthesized using pressurized vapor/condenser (PVC) methods.[14] As-synthesized BNNTs were first separated in an aqueous solution using ultrasonication methods and dispersed BNNTs were subsequently deposited on a fresh silicon substrate by spin-coating.[10,11] All of the collision measurements were performed inside a Park Systems XE-70 AFM that operates at room temperature with a 10% humidity. Silicon nitride AFM cantilevers with silicon tips (model CSG 11, NT-MDT) were employed in our study. The spring constant of each employed AFM cantilever was calibrated using the thermal tuning method[15] and was found to be in the range of 0.05–0.12 N/m. The lateral force applied to the AFM tip, L, was calculated as $L = U \cdot \alpha$, where U is the measured voltage signal in response to the horizontal motion of the reflected laser spot on the photo-detector and α is the lateral sensitivity of the cantilever,

[a)]X. Chen and M. Zheng contributed equally to this work.
[b)]Author to whom correspondence should be addressed. Electronic mail: cke@binghamton.edu. Tel.: 607-777-4782. Fax: 607-777-4620.

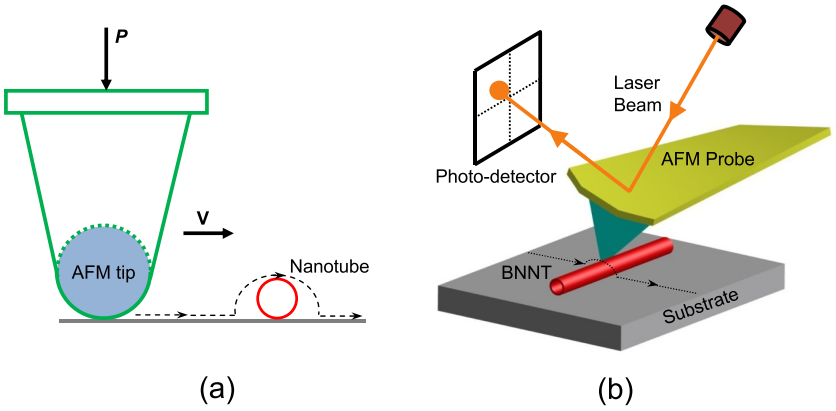

FIG. 1. (a) Schematic drawing of the lateral collision between a moving AFM probe and a standstill nanotube on a flat substrate. (b) Schematic illustration of the experimental scheme of measuring the lateral collision of a moving AFM tip onto a BNNT.

a quantity correlating the lateral force applied to the AFM tip with the horizontal motion of the laser spot on the photo-detector. Each AFM cantilever was calibrated by following a two-slope wedge method using a TGG01 silicon grating,[16] and its lateral sensitivity was found to be within the range of 0.0175–0.04 nN/mV. The tip radii of the AFM probes were estimated to be 15–25 nm based on the recorded nanotube AFM images.[17]

The red and blue (light- and dark-gray in print) curves in Figure 2(a) show, respectively, the topography and the lateral force profiles recorded in a representative BNNT collision test. The AFM tip was applied with a normal load of 0.05 nN and a velocity of 240 nm/s. The tested tube is displayed in the inset AFM image and had a cross-section height (h_0) measured to be about 2.77 nm, indicating that it was most probably a single- or double-walled tube.[10,11] The diameter of this tube (D_{nt}) was estimated to be about 2.43 nm by considering $D_{nt} = h_0 - t$,[18] in which $t = 0.34$ nm is the inter-layer distance of the B-N sheet.[14] It can be clearly seen from these two curves that the collision of the AFM tip with the nanotube resulted in a spike in the lateral force signal, corresponding to the sliding up of the AFM tip onto the nanotube surface as illustrated by the inset drawing. The measured peak lateral force (2.42 nN) was about 72% higher than the recorded lateral force when the tip only slid on the substrate. The location of the peak lateral force signal was found to be around a half-way of the measured nanotube height profile, which is marked by point A in Figure 2(a) and was also confirmed to possess the highest slope. This observation clearly indicates that the nanotube deformed under the collision of the AFM tip and the peak lateral force occurred when the AFM tip was already lifted from the substrate. Therefore, the measured lateral force equals the lateral collision force applied to the nanotube. The blue (dark-gray in print) curve in Figure 2(b) shows the corresponding slope curve of the topography profile shown in Figure 2(a). The contact angle on the tip-tube contact (as illustrated in the inset drawing) corresponding to the peak lateral force was measured to be 19.9°. Figure 2(b) also includes the slope profiles for measurements performed on the same tube with the same AFM tip moving at velocities of 40 and 2000 nm/s, respectively. Our results clearly show that the contact angle corresponding to the peak lateral force decreases with an increasing impact speed. It should be emphasized that the measured lateral collision force is due to both the tube/tip collision deformations and their topographic effects.[19,20]

When the AFM tip slid to the top of the nanotube cross-section, the corresponding lateral force (~0.83 nN) that is marked by point B in Figure 2(a) was purely due to the frictional interaction on the tip-tube contact.

Figures 3(a) and 3(b) show the respective dependences of the peak lateral collision force on the applied normal load

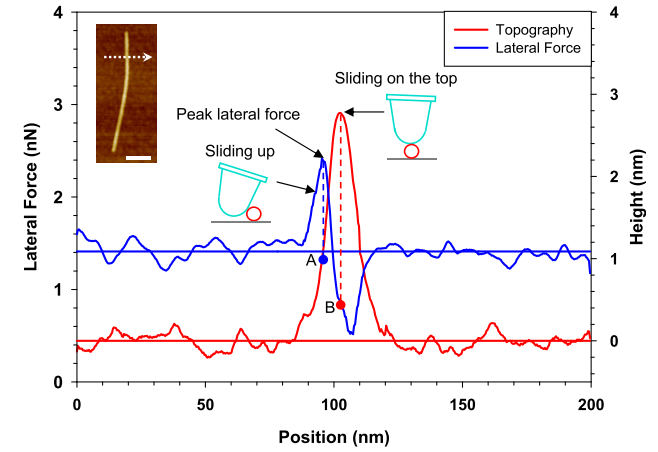

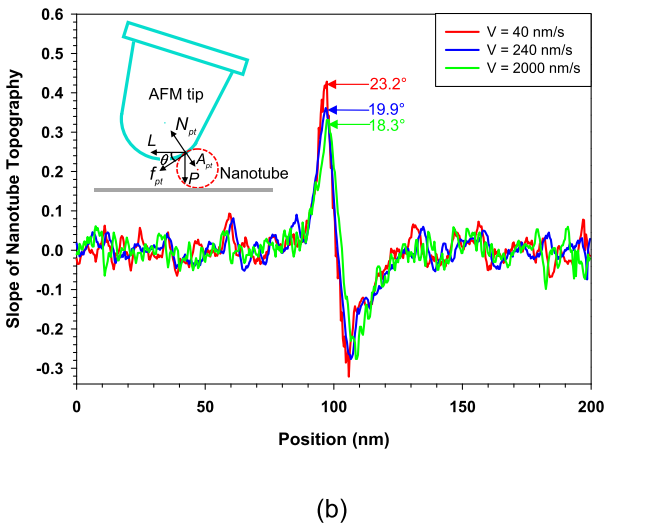

FIG. 2. (a) The topography (red curve) and lateral force (blue curve) profiles recorded in a representative BNNT collision test. The inset AFM image shows the tested tube, and the white dotted line with an arrow marks the moving trace and direction of the AFM tip. The scale bar is 100 nm. (b) The calculated nanotube topography slope profiles for the same tube shown in (a) at impact velocities of 20, 240, and 2000 nm/s, respectively. The inset drawing shows the free-body diagram of an AFM tip in a sliding-up position.

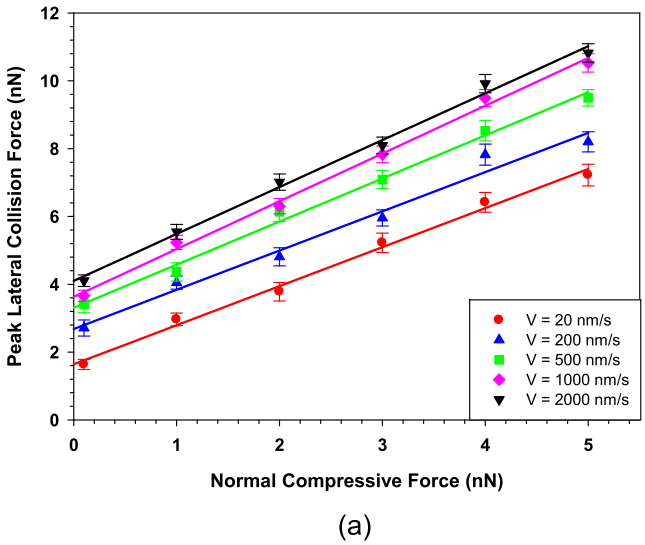

FIG. 3. The dependences of the measured peak lateral collision forces on the impact velocity and the applied normal force. The error bars were calculated based on the noise level in the measured lateral force profiles.

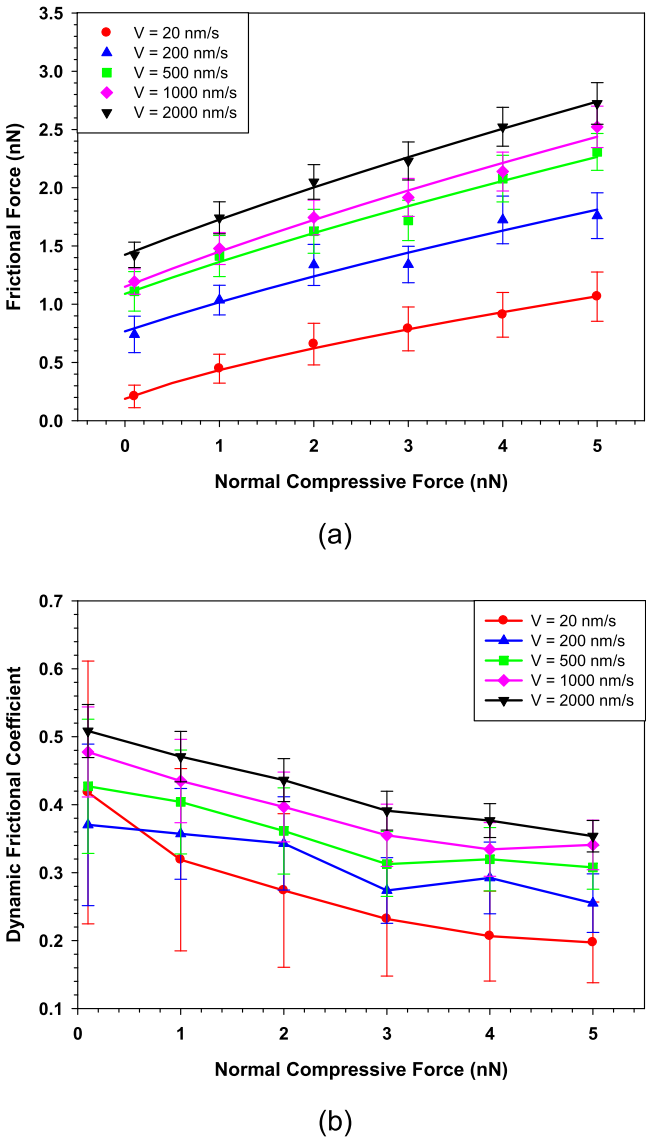

FIG. 4. (a) The dependences of the measured frictional force on the impact velocity and the applied normal compressive load. The solid lines represent the respective power-function fitting curves. (b) The calculated dynamic frictional coefficient based on the data shown in (a).

P and the impact velocity V for a BNNT of 3.48 nm in diameter, which were plotted based on the same set of data with different horizontal axes. Figure 3(a) displays a nearly linear dependence of the peak lateral collision force on the applied normal load for a velocity within the range of 20–2000 nm/s. Our data also reveal that increasing the impact velocity results in a more prominent increase of the collision force at lower velocity levels (i.e., from 20 to 500 nm/s), while a noticeably less increase at higher velocity levels (i.e., from 1000 to 2000 nm/s). Figure 4(a) shows the dependences of the frictional force when the AFM tip slid on top of the nanotube on both the applied normal load and the moving velocity for the same tube. Our data show that the frictional force increases with both the applied normal load and the moving velocity, which is consistent with the prior reports on the nanoscale frictional behavior in the literature.[21,22] The frictional force data could be well-fitted by a power function given by $C \cdot (P + A_{pt})^{2/3}$, in which A_{pt} is the adhesion force between the AFM tip and the nanotube and C is a fitting parameter. For the tested tube presented in Figures 3 and 4, the adhesion force was measured to be about 2.0 ± 0.5 nN by operating the AFM in the force modulation mode.[20] Figure 4(b) shows the corresponding dynamic frictional coefficient, μ_{pt}, on the tip-tube contact, which was calculated as $\mu_{pt} = L/(P + A_{pt})$. We can see that the dynamic frictional coefficient increases with the moving velocity, while displaying a decreasing trend with an increase of the applied normal load.

The dependence of the collision force on the impact velocity is a critical issue in the understanding of nanotube collision. Our observation of the dependence of the peak lateral collision force on the impact velocity as shown in Figure 3(b) suggests that the peak lateral collision force may reach a threshold limit with an increasing impact velocity, which is not a straight-forward expectation on the collision between two bodies. In the following discussion, we provide an explanation of our observation based on an analysis of the correlation of the lateral collision force with the dynamic frictional force and the contact angle on the tip-tube collision

contact. It is noted that the lateral collision force L is the net effect of the normal compression load applied to the tube by the AFM tip, $N_{pt,}$ and the tip-tube frictional force, f_{pt}, which is illustrated by the free-body diagram shown in Figure 2(b). Based on our measurements, the AFM tip contacts only the nanotube when the peak lateral collision force occurs. To illustrate the basic relationship among all these forces, we assume that both the AFM tip and the nanotube remain in a quasi-static state in the following analysis. The normal load applied to the AFM tip P is given by

$$P = (N_{pt} - A_{pt})(\cos\theta - \mu_{pt}\sin\theta). \quad (1)$$

The lateral collision force applied to the nanotube L is given by

$$L = (N_{pt} - A_{pt})(\sin\theta + \mu_{pt}\cos\theta) = P\frac{\tan\theta + \mu_{pt}}{1 - \mu_{pt}\tan\theta}. \quad (2)$$

Equation (2) shows that the lateral collision force depends linearly on the applied normal load, which agrees well with our experimental observation. The lateral collision force also increases with both the frictional coefficient and the contact angle. Because our measurements show that increasing the impact velocity results in an increase of the frictional coefficient and a decrease of the contact angle, the increase of the lateral collision force due to the higher frictional coefficient is partially offset by the decreasing effect of the contact angle. Therefore, our experimental observation of the effect of the impact velocity on the lateral collision force can be qualitatively explained through the above analysis based on the competition between the respective effects of the impact velocity on the frictional force and the contact angle on the tip-tube collision contact.

In this paper, the collision between individual BNNTs and AFM tips was investigated using lateral force spectroscopy techniques. The results show that the peak lateral collision force increases with the applied normal load to the AFM tip in a nearly linear manner. The frictional force on the tip-tube contact increases with the impact velocity of the AFM tip and contributes to increasing the lateral collision force. However, the corresponding tip-tube contact angle to the peak collision force decreases with an increase of the impact velocity, leading to a decrease of the lateral collision force. The interplay between the frictional force and the contact angle on the tip-tube contact is ascribed as the mechanism behind the observation that increasing the impact velocity results in a more prominent increase of the lateral collision force at low velocity levels. These results are useful to understand the collision and dynamic frictional properties of BNNTs towards realizing their impact protection applications.

This work was funded by US Air Force Office of Scientific Research Low Density Materials Program under Grant Nos. FA9550-11-1-0042 and FA9550-10-1-0451.

[1]A. Rubio, J. L. Corkill, and M. L. Cohen, Phys. Rev. B **49**, 5081 (1994).
[2]N. G. Chopra, R. J. Luyken, K. Cherrey, V. H. Crespi, M. L. Cohen, S. G. Louie, and A. Zettl, Science **269**, 966 (1995).
[3]R. Arenal, M. S. Wang, Z. Xu, A. Loiseau, and D. Golberg, Nanotechnology **22**, 265704 (2011).
[4]X. L. Wei, M. S. Wang, Y. Bando, and D. Golberg, Adv. Mater. **22**, 4895 (2010).
[5]N. G. Chopra and A. Zettl, Solid State Commun. **105**, 297 (1998).
[6]Y. Chen, J. Zou, S. J. Campbell, and G. Le Caer, Appl. Phys. Lett. **84**, 2430 (2004).
[7]D. Golberg, Y. Bando, K. Kurashima, and T. Sato, Scr. Mater. **44**, 1561 (2001).
[8]X. Blase, A. Rubio, S. G. Louie, and M. L. Cohen, Europhys. Lett. **28**, 335 (1994).
[9]Y. B. Li, P. S. Dorozhkin, Y. Bando, and D. Golberg, Adv. Mater. **17**, 545 (2005).
[10]M. Zheng, X. Chen, I.-T. Bae, C. Ke, C. Park, M. W. Smith, and K. Jordan, Small **8**, 116 (2012).
[11]M. Zheng, C. Ke, I.-T. Bae, C. Park, M. W. Smith, and K. Jordan, Nanotechnology **23**, 095703 (2012).
[12]M. Zheng, L. Zou, H. Wang, C. Park, and C. Ke, J. Appl. Phys. **112**, 104318 (2012).
[13]V. Lordi and N. Yao, J. Chem. Phys. **109**, 2509 (1998).
[14]M. W. Smith, K. C. Jordan, C. Park, J.-W. Kim, P. T. Lillehei, R. Crooks, and J. S. Harrison, Nanotechnology **20**, 505604 (2009).
[15]E.-L. Florin, M. Rief, H. Lehmann, M. Ludwig, C. Dornmair, V. T. Moy, and H. E. Gaub, Biosens. Bioelectron. **10**, 895 (1995).
[16]D. F. Ogletree, R. W. Carpick, and M. Salmeron, Rev. Sci. Instrum. **67**, 3298 (1996).
[17]C. T. Gibson, G. S. Watson, and S. Myhra, Scanning **19**, 564 (1997).
[18]T. DeBorde, J. C. Joiner, M. R. Leyden, and E. D. Minot, Nano Lett. **8**, 3568 (2008).
[19]S. Sundararajan and B. Bhushan, J. Appl. Phys. **88**, 4825 (2000).
[20]M. A. J. Lievonen, Ultramicroscopy **109**, 825 (2009).
[21]H.-C. Chiu, S. Dogan, M. Volkmann, C. Klinke, and E. Riedo, Nanotechnology **23**, 455706 (2012).
[22]M. Lucas, X. Zhang, I. Palaci, C. Klinke, E. Tosatti, and E. Riedo, Nature Mater. **8**, 876 (2009).